Supporting Information

Insight into the Origin of SARS-CoV-2 through Structural Analysis of Receptor Recognition: A Molecular Simulation Study

Jixue Sun[a], Meijiang Liu[a] & Na Yang[a,*]

[a]State Key Laboratory of Medicinal Chemical Biology, College of Pharmacy and Key Laboratory of Medical Data Analysis and Statistical Research of Tianjin, Nankai University, Tianjin 300353, China;

[*]To whom correspondence may be addressed: E-mail: yangnaNKU@nankai.edu.cn

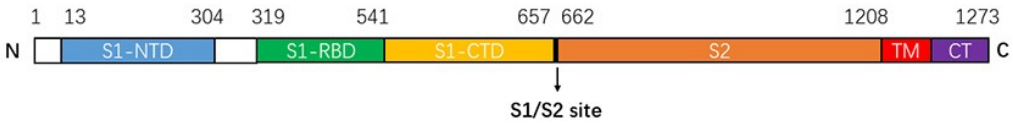

Figure S1. A schematic drawing of S protein domain organization.

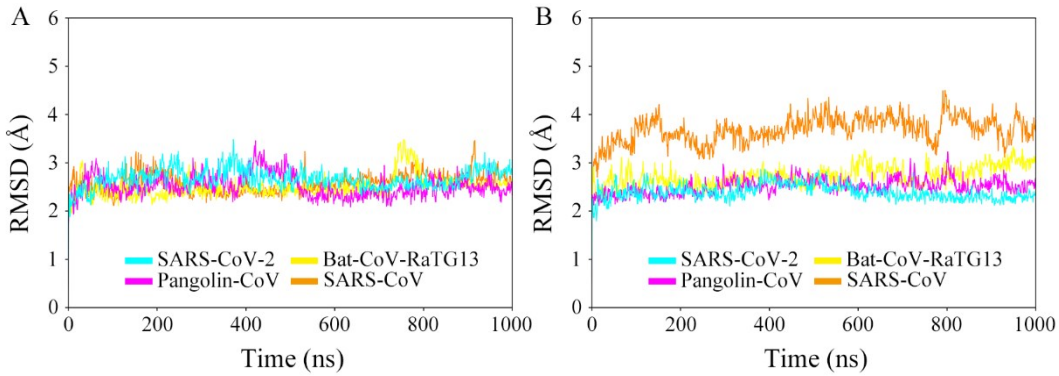

Figure S2. Time evolutions of RMSD for (A) hACE2 and (B) RBD. SARS-CoV-2, Pangolin-CoV, Bat-CoV-RaTG13, and SARS-CoV are shown in cyan, magenta, yellow, and orange, respectively.

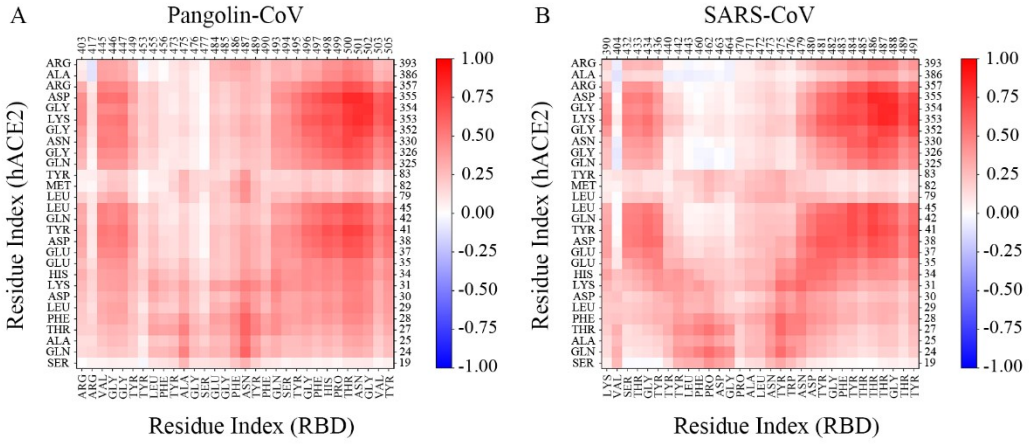

Figure S3. Dynamic cross-correlation maps for the (A) Pangolin-CoV and (B) SARS-CoV systems. The color scale is shown on the right changing from red (highly positive correlations) to blue (highly negative correlations).

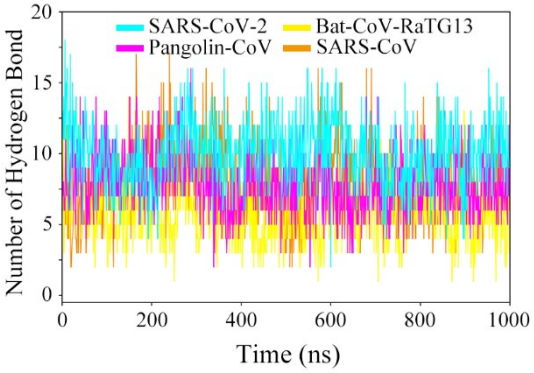

Figure S4. Time evolutions of the number of hydrogen bonds between RBD and hACE2.

Table S1 Averaged values of the solvent accessibility surface area of the residues at the RBD-hACE2 interface for the simulated systems during the last 200 ns MD simulations.

RBD	SARS-CoV-2	Pangolin-CoV	Bat-CoV-RaTG13	SARS-CoV
SASA ($Å^2$)	1950.42	2169.72	2313.32	2018.32

Table S2 Decomposed binding free energies of the residues at the interface of RBD and hACE2 in the four systems.

Residue	2019-nCoV	Pangolin-CoV	Bat-CoV-RaTG13	SARS-CoV
R/R/T403/K390	-3.99 ± 1.29	0.00 ± 0.55	0.28 ± 0.11	1.22 ± 0.48
K/R/K417/V404	-0.52 ± 1.58	-2.72 ± 1.92	1.74 ± 1.88	-0.11 ± 0.05
V/V/E445/S432	0.15 ± 0.06	0.02 ± 0.08	0.49 ± 0.22	0.45 ± 0.12
G/G/G446/T433	0.04 ± 0.43	-0.22 ± 0.34	0.18 ± 0.05	0.25 ± 0.08
G/G/G447/G434	0.28 ± 0.10	-0.11 ± 0.18	0.16 ± 0.08	0.03 ± 0.12
Y/Y/F449/Y436	-0.84 ± 0.61	-0.02 ± 0.43	-0.08 ± 0.15	-1.40 ± 0.76
Y/Y/Y453/Y440	0.32 ± 0.41	0.15 ± 0.30	-0.14 ± 0.39	0.30 ± 0.35
L/L/L455/Y442	-2.11 ± 0.36	-2.12 ± 0.35	-1.70 ± 0.42	-1.83 ± 0.69
F/F/F456/L443	-2.33 ± 0.40	-2.44 ± 0.44	-2.83 ± 0.49	-0.66 ± 0.17
Y/Y/Y473/F460	-0.04 ± 0.13	-0.07 ± 0.16	-0.68 ± 0.47	-0.01 ± 0.08
A/A/A475/P462	-0.72 ± 0.53	-1.30 ± 0.78	-2.46 ± 1.41	-2.94 ± 0.51
G/G/G476/D463	-0.26 ± 0.31	-0.62 ± 0.43	-1.55 ± 0.97	-0.63 ± 1.05
S/S/S477/G464	0.00 ± 0.13	0.08 ± 0.20	-0.26 ± 0.61	-0.01 ± 0.04
E/E/T484/P470	0.80 ± 0.26	1.19 ± 0.94	0.27 ± 0.09	0.12 ± 0.03
G/G/G485/A471	0.25 ± 0.08	0.20 ± 0.09	0.38 ± 0.13	0.14 ± 0.05
F/F/L486/L472	-3.25 ± 0.79	-2.74 ± 1.14	-1.61 ± 1.35	-0.87 ± 0.67
N/N/N487/N473	-1.07 ± 0.62	-1.29 ± 0.88	-0.23 ± 0.61	-1.09 ± 0.91
Y/Y/Y489/Y475	-1.10 ± 0.50	-1.23 ± 0.68	-2.12 ± 0.78	-1.62 ± 0.91
F/F/Y490/W476	0.06 ± 0.07	0.04 ± 0.18	0.30 ± 0.10	-2.31 ± 1.05
Q/Q/Y493/N479	-4.87 ± 1.33	-4.66 ± 1.36	-2.23 ± 0.84	-5.34 ± 1.49
S/S/R494/D480	0.37 ± 0.21	0.41 ± 0.21	0.05 ± 0.34	9.43 ± 1.49
Y/Y/Y495/Y481	-0.22 ± 0.28	0.01 ± 0.27	-0.19 ± 0.19	-1.87 ± 0.41
G/G/G496/G482	-2.27 ± 0.51	-1.40 ± 0.79	-0.62 ± 1.32	-0.66 ± 0.36
F/F/F497/F483	-0.36 ± 0.24	-0.50 ± 0.20	-0.23 ± 0.15	-0.49 ± 0.12
Q/H/Y498/Y484	-6.75 ± 0.92	-3.01 ± 1.00	-1.37 ± 0.95	-2.62 ± 0.52
P/P/P499/T485	-0.22 ± 0.09	-0.30 ± 0.09	-0.05 ± 0.09	0.21 ± 0.16
T/T/T500/T486	-1.10 ± 0.80	-1.61 ± 0.81	-0.13 ± 0.53	-0.92 ± 0.71
N/N/D501/T487	-4.28 ± 0.99	-3.13 ± 0.69	-3.66 ± 1.39	-3.37 ± 0.52
G/G/G502/G488	-1.73 ± 0.38	-1.53 ± 0.43	-1.49 ± 0.40	-1.30 ± 0.37
V/V/V503/T489	-0.27 ± 0.13	-0.31 ± 0.24	-0.88 ± 0.53	-0.36 ± 0.21
Y/Y/H505/Y491	-3.60 ± 0.68	-3.44 ± 0.74	-2.74 ± 0.98	-3.65 ± 0.78

All binding free energies are given in kcal/mol.